Applied Surface Science 266 (2013) 395–399

Contents lists available at SciVerse ScienceDirect

Applied Surface Science

journal homepage: www.elsevier.com/locate/apsusc

The fabrication of controlled coral-like Cu_2O films and their hydrophobic property

Yanbo Ding[a,c], Yao Li[b], Lili Yang[d], Zhenyu Li[b], Wuhong Xin[b], Xin Liu[b], Lei Pan[b], Jiupeng Zhao[a,*]

[a] School of Chemical Engineering and Technology, Harbin Institute of Technology, Harbin, 150001, China
[b] Center for Composite Materials and Structures, Harbin Institute of Technology, Harbin, 150080, China
[c] School of Science, Harbin Institute of Technology, Harbin, 150001, China
[d] School of Transportation Science and Engineering, Harbin Institute of Technology, Harbin, 150090, China

ARTICLE INFO

Article history:
Received 29 August 2012
Received in revised form
22 November 2012
Accepted 10 December 2012
Available online 20 December 2012

Keywords:
Coral-like
Contact angles
Superhydrophobic
Electrodeposition

ABSTRACT

In this paper, we report on the nanostructured Cu_2O film with controllable coral-like morphology in the presence of $CuCl_2$ by electrodeposition without using any performed template. Four types of patterned Cu_2O films including grains-like, agaric-like, frutex-like and coral-like films were achieved by governing the time or additive. The coral patterned Cu_2O film is for the first time found here. Additionally, possible growth mechanism for multi-patterned Cu_2O is discussed via preferential growths induced by selective absorption of Cl^- ions in the present reaction system. The resulting pattered films displayed tunable hydrophobic and even superhydrophobic properties owing to their special surface with micro-/nanostructures after simple surface modification. These experimental results prove a versatile and facile strategy for Cu_2O films with special and complex architectures which may highlights their potential applications in self-cleaning equipment due to the improved surface activity.

1. Introduction

Water-repellent and hydrophobic properties of many biological entities have been acknowledged for thousands of years. Many plants and arthropods are known for having water-resistant exteriors, such as lotus leaves, mosquito and water spider. With the advancement of microscopy in the last few decades, multiple microstructures have been found on these surfaces, which vigorously stimulated the research on making superhydrophobic surfaces. The unique functionalities of the natural organism were attributed to the combination of special hierarchical micro-/nanostructures surface and low surface-free energy materials covering the surfaces [1]. Inspired by this, various techniques to synthesize superhydrophobic surfaces have been developed, including a rough polymer surface by argon plasma etching [2], a hierarchical micro-/nanostructures film by the wet chemical method [3], superhydrophobic rough surfaces by electrochemical methods [4], polymer patterns by the polymerization on the etched silicon substrate [5], stable bionic superhydrophobic surfaces by solution-immersion process [6], porous films by electron irradiation or template techniques [7].

Since the morphological diversity of inorganic micro-/nanomaterials has a significant impact on their functional diversification and potential applications. Thence, control of the unusual shapes and size of materials is stimulating worldwide interests in areas of materials science [8–10], including prepare glassy coatings for tiles based on copper pigment by a conventional industrial process [11]. Particularly, over the past decade, one- and two dimensional (1D and 2D) nanostructures (nanowires, nanoribbon, nanorods nanobelts) have been a focus of extensive research due to their unique optical, electrical and mechanical properties [12–16]. Therefore, tremendous efforts have been dedicated to investigate the preparation of 1D or 2D building blocks into special three-dimensional architectures with the use of surfactants or templates, because such configurations may not only provide the needs of many novel technologies based on nanoscale machines and devices, but also give insight into the construction of micro-/nanoscale devices.

Cuprous oxide (Cu_2O) is a naturally p-type semiconductor with an optical gap of 1.95–2.2 eV at room temperature, which could be used in the top cell of a multi-junction solar cell or as the host material for an intermediate band solar cell due to the value of its energy gap and the low production cost. Contemporarily, Cu_2O has received a great attention because of its potential applications in solar energy conversion [17–19], catalysis [20] and gas sensors [21]. In this paper, we present a more detailed study on the effects of additive on the Cu_2O morphology prepared by

* Corresponding author. Tel.: +86 45186403767; fax: +86 45186403767.
E-mail address: jiupengzhao@126.com (J. Zhao).

0169-4332/$ – see front matter © 2012 Elsevier B.V. All rights reserved.
http://dx.doi.org/10.1016/j.apsusc.2012.12.043

electrodeposition and characterized for their structural, morphological and contact angles (CAs) behavior. We established an environmentally benign template-free electrodeposition approach to fabricate three-dimensional Cu_2O architectures with various morphologies in the presence of $CuCl_2$, including agaric-like, frutex-like and coral-like Cu_2O film. Herein, tunable hydrophobic/superhydrophobic surfaces of Cu_2O architectures were realized based on their special surface micro-/nanostructures. To the best of our knowledge, the controllable coral-like Cu_2O film has never been reported by any chemical synthesis method. The findings in this work are attractive for their merits such as simplicity, safety, environmentally benign, commercial feasibility, and good potential for self-cleaning utensils.

2. Experimental

2.1. Materials and preparation

Cu_2O was grown potentiostatically in a three-electrode system controlled by CHI-660D potentiostat. ITO (1 cm × 4 cm) was used as the working electrode with Pt parallel counter electrode and a saturated calomel reference electrode (SCE). ITO (R_s = 15 Ω) were all commercially available products, and washed with acetone, ethanol, and ultrapure water under sonication for 20 min (respectively) before use. The starting materials used were cupric sulfate ($Cu_2SO_4{\cdot}5H_2O$), lactic acid ($C_3H_6O_3$), sodium hydroxide (NaOH), cupric chloride ($CuCl_2$). All these chemicals are analytical reagents used without further purification. Water used in all experiments was purified with a resistivity greater than 18 ΩM/cm. The temperature was kept at 60 °C controlled by a precision 280 water bath during the experiments. After deposition, the films were rinsed with copious amounts of ultrapure water, dried at room temperature.

2.2. Characterization

The phase composition of the crystalline structure of products was analyzed by X-ray diffraction (XRD) on a Phillips X'Pert diffractometer equipped with Cu Kα radiation at a scan rate of 5° min^{-1}. The morphologies of the products were performed using a QUANTA 200F SEM (FEI, American) scanning electron microscope operating at an accelerating voltage of 30 kV. The samples were sputter-coated with gold before examination. Water contact angles were measured on a drop-shape analyses system (JC2000C3, ZhongChen Precision, Shang Hai) at ambient temperature. The equilibrium water contact angle (CA) was measured with a fixed needle supplying a water drop of 5 μL. Five different points on each sample were investigated.

3. Result and discussion

3.1. The XRD pattern of as-prepared Cu_2O films

Fig. 1 shows the XRD spectrum of the Cu_2O film without additive and Cu_2O architectures prepared with additive. All peaks can be clearly indexed as a pure cubic phase of Cu_2O and matched well with the reported data (JCPDS card File No. 05-0667. space group *Pn*-3*m* (2 2 4), a_0 =0.427 nm). The sharp diffraction peaks indicate a high purity and crystallinity of the final product. Obviously, The diffraction peaks corresponding to planes (1 1 0), (1 1 1), (2 0 0), (2 2 0) and (3 1 1), which provide a clear evidence for the formation of cuprous oxide. However, the intensity of the peaks is clearly different as shown in Fig. 1. The as-product Cu_2O without additive has the highest peak at the (2 0 0) orientations, while the Cu_2O favor the (1 1 1) orientations prepared with additive, which may due to the

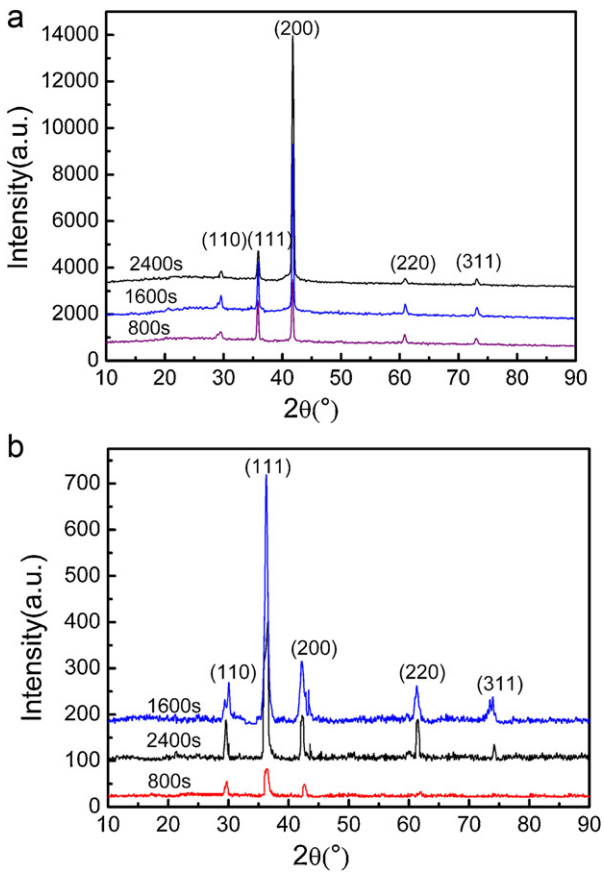

Fig. 1. XRD spectrum of the Cu_2O film (a) without additive, (b) with additive.

Cl^- ions adsorb onto the positive polar face of some crystal plane and change the crystal growth. The details will be discussed in the following part.

3.2. Morphologies of different Cu_2O films

The electrolyte solution consisted of 0.4 M $CuSO_4$ and 3 M lactic acid, the pH of the solution was adjusted to 9 by 8 wt% NaOH solution, the electrodeposition was conducted at applied potential of −0.35 V in a three-electrode arrangement.

The Cu_2O films of different electrodeposition time demonstrated rather different surface morphologies as shown in Fig. 2, which illustrate the evolving growth steps of Cu_2O films performed under deferent time. The Cu_2O film electrodeposited of 800 s results in the growth of grains uniformly distributed over the substrate shown in Fig. 2(a) (d). The grains have a shape of nanograins with diameters of <200 nm, heights of <50 nm. The Cu_2O film in plane view presented larger grained morphologies with deposition time increased to 1600 s as shown in Fig. 2(b) (e), which also exhibit granular structure with small grains and their grain sizes between 200 nm to 400 nm. The Cu_2O films display uniform grains and well-defined grain boundaries under 2400 s shown in Fig. 2(c) (f), and the crystalline grow up to about 1 um. Obviously, the individual grains become much bigger compared to those prepared before, which exhibiting a considerable surface roughness distributing all over the surface. Absolutely, their surface roughness was enhanced apparently as the deposition time extended. Simultaneously, the XRD pattern clearly shows that the intensity of the peaks was higher as the deposition time increase (Fig. 1). This result implies that such Cu_2O crystallites grow to the larger size continuously after they nucleated.

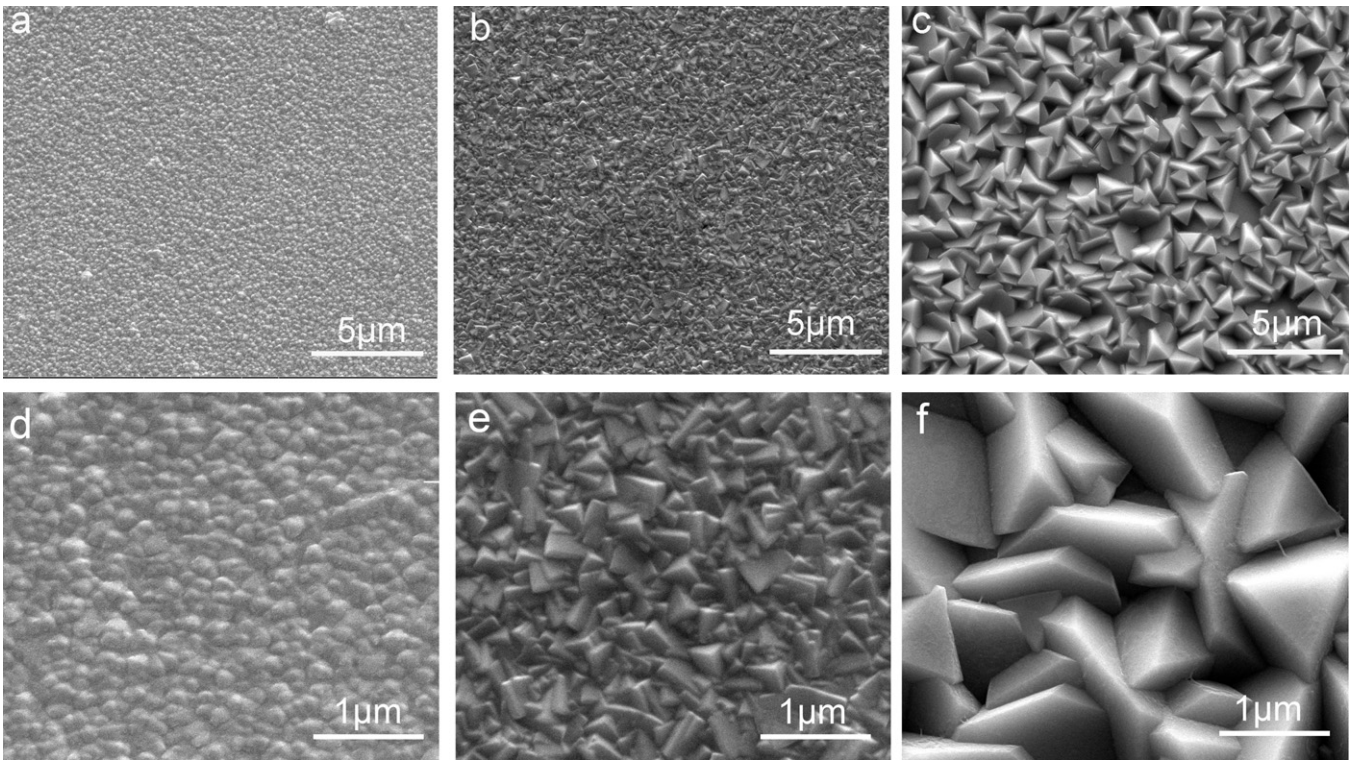

Fig. 2. The surface morphologies of Cu_2O films at different electrodeposited time. (a) 800 s, (d) magnified, (b) 1600 s, (e) magnified, (c) 2400 s, (f) magnified.

The deposition was executed at −0.16 V after 0.15 M $CuCl_2$ added into the aforementioned solution. The Cu_2O films at different deposition time demonstrated rather different surface morphologies as shown in Fig. 3. Apparently, the morphologies of the Cu_2O films are significantly affected by the additive compared to the as-prepared Cu_2O film (Fig. 2). A large number of isolated papilla uniformly distributed over the substrate with an average diameter about 2–3.5 μm at 800 s (Fig. 3a). A close up micrograph observation revealed that the single papilla possessed an elegant appearance, similar to agaric in nature (Fig. 3b).

The low magnification image shows the uniformity of the frutex-like Cu_2O nanostructure prepared under 1600 s (Fig. 3c). Interestingly, the frutex was constructed by a large number of separated "nanorods". Fig. 3d shows a high-magnification image of frutex-like Cu_2O films. It is obviously seen that the frutex-like Cu_2O microcrystals aggregated by nanorods with a length of about 4–5 μm and a diameter of 500 nm, which, similar to wattles assemble as frutex in nature. Meanwhile, many spacing among these "nanorods" may favor the diffusion of small molecules in practical catalysis application. The Cu_2O products with nanorods grow all over the substrate as the deposition time extends to 2400 s as show in Fig. 3e, which similar as coral in nature. More interesting, there is thorn epitaxially grow perpendicular onto the stem. Among them, the primary structures are the longest. The whole length of the Cu_2O stems reach up to more than 5 μm shown in Fig. 3f and the diameter is about 200 nm.

3.3. The wettability and formation mechanism of the Cu_2O architectures

Fig. 4 shows the captured micrographs of water droplet on the surface of Cu_2O film deposited on ITO substrates under different time with or without additive. It is obviously seen that CAs increase from $69 \pm 1.38^\circ$ to $86 \pm 0.75^\circ$ then to $95 \pm 0.72^\circ$ as the deposition time increase from 800 s, 1600 s to 2400 s. Compared to the Cu_2O sample prepared without additive, the CAs was found to increase from $105 \pm 0.74^\circ$ on agaric-like Cu_2O film to $148 \pm 0.71^\circ$ for frutex-like one then to $169 \pm 0.58^\circ$ for coral-like film, indicating the surface change from hydrophobicity to superhydrophobicity with the deposition time increase. More interesting, the CAs of Cu_2O film with coral-like pattern was higher than 74° compared to those fabricated without additive under the same deposition time of 2400 s (Fig. 4c, f), which suggested that the additive can basically change the morphology of Cu_2O film to be a typical self-cleaning surface.

The aforementioned results verified that the surface wettability of Cu_2O films was converted from hydrophobicity to superhydrophobicity via surface modification by simply change the deposition time or additive. Some researchers reported that the preferential adsorption of molecules and ions in solution to different crystal faces directed the growth of micro-/nanostructures into various shapes by controlling the growth rates along different crystal axes [22–24]. We speculated that Cl^- ions play a significant role in controlling the morphology of the Cu_2O films considering the material used in our experiment. Consequently, the formation mechanism of Cu_2O morphologies might be attributed to the adsorption of Cl^- ions on the positive polar face of some crystal plane by electrostatic force, which in turn changed the surface energies of different crystal planes and hindered the crystal growth perpendicular to the plane of lower surface energy, resulting in the changes of the Cu_2O crystal morphology. More importantly, special surface combination of micro-/nanostructures of Cu_2O configurations could trap air in the spacing among particles. This led to the significant decrease in the contact area between water and the surface protrusions of nanorodes, resulting in hydrophobicity or even superhydrophobicity property.

Therefore, our results demonstrated that the superhydrophobicity of the coral-like Cu_2O resulted from the special combination of micro-/nanostructures hierarchical. And two well established

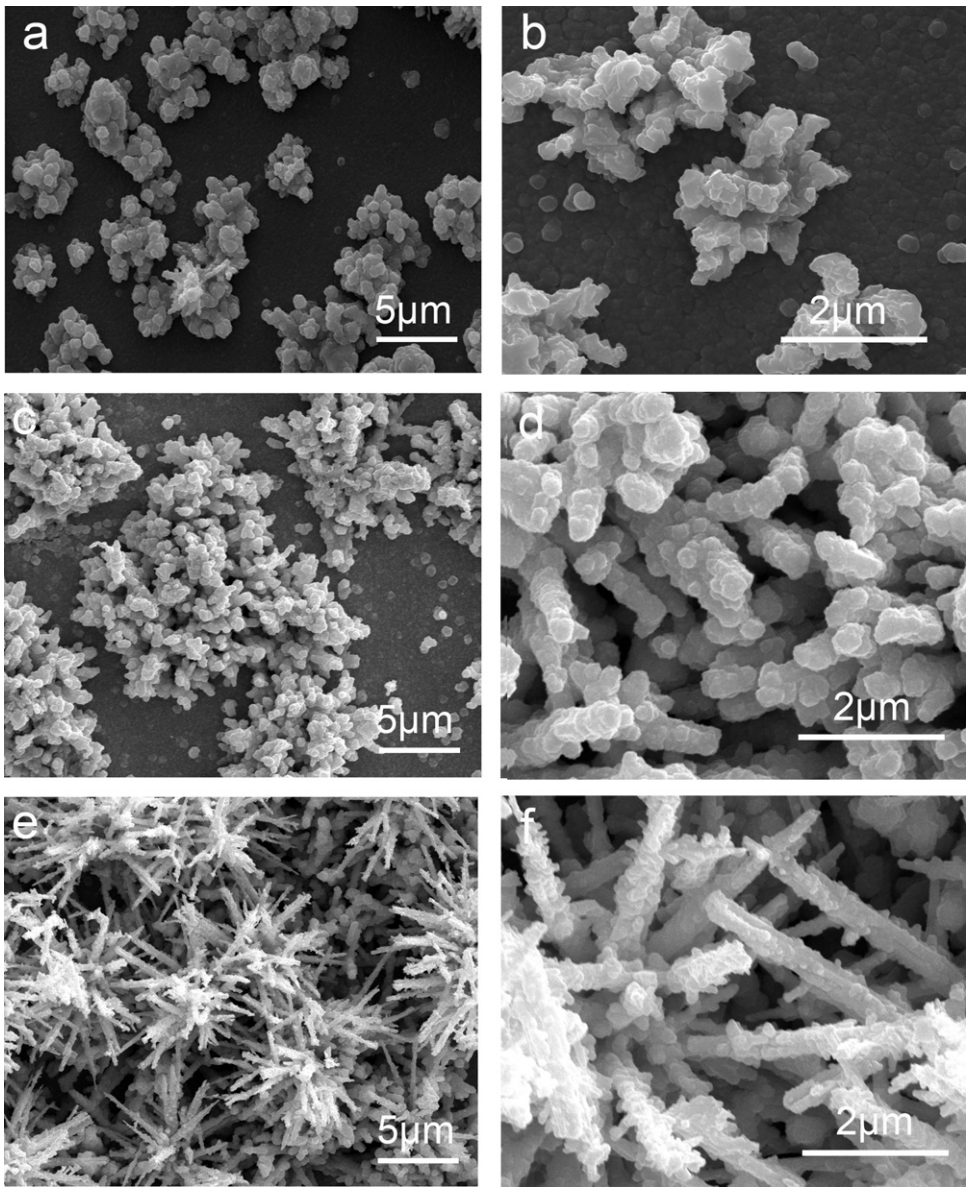

Fig. 3. Morphologies of Cu_2O films prepared with additive at different electrodeposited time. (a) 800 s, (b) magnified, (c) 1600 s, (d) magnified, (e) 2400 s, (f) magnified.

models are generally used for describing the wettability of a rough surface. When a water droplet can dip into the groove on the surface of film, Wenzel gave a wettability description by [25].

$$\cos\theta_r = r\cos\theta \quad (1)$$

where r is the roughness factor (the ratio of total surface area to the projected area on the horizontal plane), θ_r and θ are the CAs of a rough surface and a native surface, respectively. Eq. (1) describes the fact that the surface roughness enhances the hydrophilicity of a hydrophilic surface ($\theta < 90^\circ$) and hydrophobicity of a hydrophobic surface ($\theta > 90^\circ$). Here θ is 95° and 169° before and after modification under 2400 s, which indicates that this hierarchical structure has the largest roughness. The Wenzel mode well demonstrated why the surfaces are more hydrophobic after modification.

Particularly, when a water droplet added onto the chemically modified frutex-like or coral-like film, air can be trapped in interstices or corrugations that are produced in the micro-/nanostructures architecture. In this case, another model presented by Cassie and Baxter can be used to explain [26]

$$\cos\theta_r = f_1\cos\theta - f_2 \quad (2)$$

where $f_1(=1-f_2)$ and f_2 are the area fractions of a water droplet in contact with the surface and with air on the surface, respectively. Since the measured water CAs of the flat Cu_2O surface and the coral-like film modified are 95° and 169° respectively, f_2 for the as-prepared surface is calculated to be 0.98. For the frutex-like films obtained by electrodeposition, its water CAs after modification is 148° and corresponding $f2$ is only 0.86. From above analysis, it reveals that the synthesized hierarchical structured surface produces large amount of air traped in the micro-/nanostructures composed surface and that the strong superhydrophobicity of the bionic surface is mainly account for the unique hierarchical architecture.

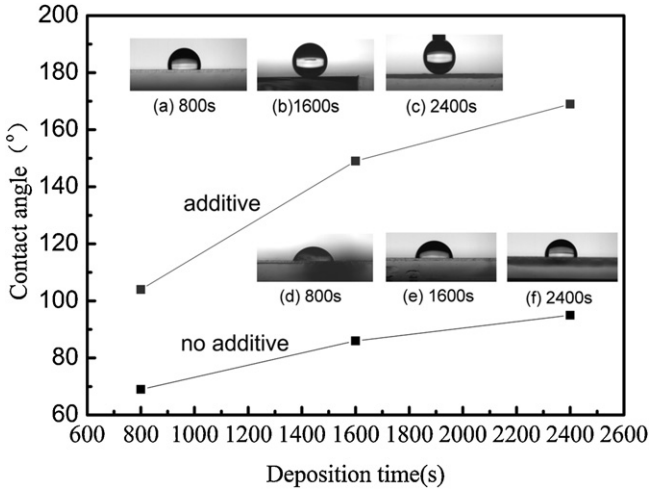

Fig. 4. The captured micrographs of water droplet on the surface of Cu_2O deposited on ITO substrates and their contact angles as the deposition time. (a) 800 s, $105 \pm 0.74^\circ$, (b) 1600 s, $148 \pm 0.71^\circ$, (c) 2400 s, $169 \pm 0.58^\circ$ with additive; (d) 800 s, $69 \pm 1.38^\circ$,(e) 1600 s, $86 \pm 0.75^\circ$and (f) 2400 s, $95 \pm 0.72^\circ$without additive.

4. Conclusions

In summary, we developed a new green synthetic route to fabricate four types of special Cu_2O architectures by electrodeposition. The morphology of Cu_2O configurations on the substrate was diversified by governing the deposition time or additive. The grains grow larger as the deposition time increasing. The shape of Cu_2O changed progressively from agaric-like to frutex-like and then to coral-like as the deposition time extended with additive. The average contact angles increased gradually from about $105 \pm 0.74^\circ$on agaric-like Cu_2O film to $148 \pm 0.71^\circ$for frutex-like one then to $169 \pm 0.58^\circ$for coral-like film. The surface hydrophobicity/superhydrophobicity was achieved on the modified Cu_2O films due to the combination of uniform micro-/nanostructure. It is expected that this promising approach can be applied to the morphosynthesis of functional Cu_2O-based materials for potential applications as advanced catalysts, clean surface and sensors.

Acknowledgment

We thank National Natural Science Foundation of China (No. 90916020, 51174063, 51102068), the Fundamental Research Funds for the Central Universities (HIT.ICRST.2010001) and Sino-German joint project (GZ550).

References

[1] X. Gao, L. Jiang, Nature 432 (2004) 36.
[2] L.C. Gao, T.J. McCarthy, Langmuir 24 (17) (2008) 9184.
[3] Y. Li, X.J. Huang, S.H. Heo, C.C. Li, Y.K. Choi, W.P. Cai, S.O. Cho, Langmuir 23 (2007) 2169.
[4] M. Nicolas, F. Guittard, S. Géribaldi, Langmuir 22 (2006) 3081.
[5] F. Xia, L. Feng, S. Wang, T. Sun, W. Song, W. Jiang, L. Jiang, Advanced Materials 18 (2006) 432.
[6] S. Wang, L. Feng, L. Jiang, Advanced Materials 18 (2006) 767.
[7] E.J. Lee, H.M. Lee, Y. Li, L.Y. Hong, D.P. Kim, C.S. O. Macromolecular Rapid Communications 28 (2007) 246.
[8] J.S. Son, X.D. Wen, J. Joo, J. Chae, S. Baek, K. Park, J.H. Kim, K. An, J.H. Yu, S.G. Kwon, S.H. Choi, Z. Wang, Y.W. Kim, Y. Kuk, R. Hoffmann, T. Hyeon, Angewandte Chemie International Edition 48 (2009) 6862.
[9] C. Chen, W. Chen, J. Lu, D. Chu, Z. Huo, Q. Peng, Y. Li, Angewandte Chemie International Edition 48 (2009) 4818.
[10] D. Portehault, C. Sophie, N. Nassif, E. Baudrin, J.P. Jolivet, Angewandte Chemie International Edition 47 (2008) 6442.
[11] J.J. Reinosa, et al., Inorganic hydrophobic coatings: surfaces mimicking the nature, Ceramics International (2012).
[12] R. Selvin, H.L. Hsu, N.S. Arul, S. Mathew, Advanced Materials 2 (2010) 60.
[13] Y. Wang, H. Yang, Journal of Chemical Engineering 147 (2009) 72.
[14] C.K. Chan, H. Peng, R.D. Twesten, K. Jarausch, X.F. Zhang, Y.F. Cui, Nano Letters 7 (2007) 492.
[15] Y. Zhou, Science of Advanced Materials 2 (2010) 359.
[16] D.P. Singh, N. Ali, Advanced Materials 2 (2010) 296.
[17] Y.H. Lee, I.C. Leu, S.T. Chang, C.L. Liao, K.Z. Fung, Electrochimica Acta 50 (2004) 553.
[18] A.S. Reddy, G.V. Rao, S. Uthanna, P.S. Reddy, Materials Letters 60 (2006) 1617.
[19] X. Li, F. Tao, Y. Jiang, Z. Xu, Journal of Colloid and Interface Science 308 (2007) 460.
[20] H. Yang, J. Ouyang, A. Tang, Y. Xiao, X. Li, X. Dong, Y. Yu, Materials Research Bulletin 41 (2006) 1310.
[21] S.T. Shishiyanu, T.S. Shishiyanu, O.I. Lupan, Sensors Actuators B 113 (2006) 468.
[22] M.J. Siegfried, K.S. Choi, Angewandte Chemie International Edition 44 (2005) 3218.
[23] M.J. Siegfried, K.-S. Choi, Advanced Materials 16 (2004) 1745.
[24] M.J. Siegfried, K.-S. Choi, Journal of the American Chemical Society 128 (2006) 10356.
[25] R.N. Wenzel, Journal of Physical and Colloid Chemistry 53 (1949) 1446.
[26] A.B.D. Cassie, S. Baxter, Transactions of the Faraday Society 40 (1944) 546.